JOURNAL OF RESEARCH of the National Bureau of Standards—D. Radio Propagation

Vol. 64D, No. 4, July–August 1960

Diffraction by Smooth Conical Obstacles [1]

H. E. J. Neugebauer [2] and M. P. Bachynski

(November 24, 1959; revised January 11, 1960)

Expressions obtained earlier [1, 2] [3] for the calculation of diffraction due to conducting obstacles with smooth cylindrical surfaces, are generalized to oblique incidence and to surfaces of conical shape. The derivation is based on a generalized concept of the Green's function and on the use of corrective factors that take the same place as corrections introduced by other authors into the theory of diffraction by apertures. The final expressions for conical obstacles and oblique incidence are very similar to those for cylindrical obstacles. The results are compared with scale model measurements.

1. Introduction

Kirchhoff's theory for the solution of diffraction problems can be generalized to be applicable to the case of scattering by cylindrical obstacles with smooth surfaces. In two recent publications [1, 2] it has been shown that the predictions of this theory are in good agreement with experiments. In addition, J. R. Wait and A. M. Conda [3] have derived numerical results from a different theory which are also in agreement with our own experimental and theoretical conclusions.

An object of the present paper is a further generalization of our investigations to conical obstacles and oblique incidence. Another object is a more thorough justification of the theoretical procedure used previously [1].

2. Basic Theory

In figure 1, T_1 represents a transmitter, T_2 a receiver, and Z a perfectly conducting obstacle of cylindrical shape between the two stations. Green's theorem (1) can be used to calculate the field E at receiver T_2.

$$E=-\frac{1}{4\pi}\iint\left(G\frac{\partial E'}{\partial n}-E'\frac{\partial G}{\partial n}\right)dS. \tag{1}$$

The integration is extended over the entire plane Ξ separating the two stations, the normal n points inwards, E' is the radiation at the plane Ξ and G is Green's function. If the field E' and Green's function were rigorously known the field E could be rigorously calculated from (1). Neither E' nor G are known, but approximate values can be obtained by the following reasoning.

Incident radiation travels directly from T_1 to V. In addition, some radiation is reflected at point S_1 of the obstacle and reaches point V. The sum of these two radiations is used as E' in eq (1).

Such a procedure obviously involves two approximations: (a) Strictly speaking the radiation reflected from a curved surface cannot be calculated from geometrical optics. However, the curvature of the obstacle is assumed to be small enough so that geometrical optics is a permissible approximation. (b) As is typical for Kirchhoff's theory, the unperturbed incident field is substituted for the true field in the plane of integration.

---

[1] Contribution from Research Laboratories, RCA Victor Company, Ltd., Montreal, Canada.
[2] Present address: 59 Fuller Ave., P.O. Box 176, Webster, N.Y.
[3] Figures in brackets indicate the literature references at the end of this paper.

Turning next to the discussion of Green's function, we recall that G is the field at T_2 when a unit source of radiation is located at V. When the effect of obstacles is neglected

$$G=\frac{e^{-jkR_2}}{R_2} \tag{2}$$

where R_2 is the distance from V to T_2, and $k=2\pi/\lambda$ is the wave number. This basic form of Green's function is used for the solution of many simple diffraction problems.

The correct form of Green's function must, however, satisfy the boundary conditions at the obstacle Z [4 to 7]. In the case of plane obstacles the image of V is added as a virtual source of radiation. In the present case, an approximate form of Green's function is obtained by adding to the expression of eq (2), the reflected radiation traveling from V via S_2 to T_2. A necessary precondition for such a procedure is that geometrical optics is a sufficiently accurate approximation for the calculation of the reflected radiation.

Another justification for the use of this approximation follows from the property of Green's function to be symmetrical in the coordinates of V and T_2. Placing a unit source of radiation at T_2 and calculating its field at V is essentially the same problem as calculating the incident field at V due to a source at T_1. Hence, it is reasonable to use the same method for the determination of E' and G, thereby automatically satisfying the reciprocity theorem.

Summarizing the preceding considerations we state that

$$E'=\frac{e^{-jkR_1}}{R_1}+\rho\ \mathrm{Div}_1\frac{e^{-jk[R'_1+r_1]}}{R'_1+r_1} \tag{3}$$

$$G=\frac{e^{-jkR_2}}{R_2}+\rho\ \mathrm{Div}_2\frac{e^{-jk[R'_2+r_2]}}{R'_2+r_2} \tag{4}$$

can be expected to be useful approximations for the field in plane Ξ and for Green's function.

The meaning of the distances R_1, R'_1, r_1, . . . can be taken from figure 1. The symbols Div_1 and Div_2 denote divergence factors [8] that take care of the loss of intensity when radiation is reflected by a curved surface. The factor ρ is different for vertical and horizontal polarization. It will be further discussed at the end of this section and in section 3.2(d).

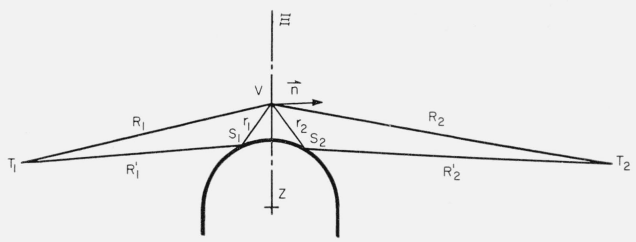

FIGURE 1. *Notation for diffraction by a cylindrical obstacle.*

In applying equation (1) use will be made of the inequality

$$kr\gg 1 \tag{5}$$

so that the derivatives of E' and G are

$$\frac{\partial E'}{\partial n}=-jk\frac{e^{-jkR_1}}{R_1}\cos(R_1,n)-jk\ \rho\ \mathrm{Div}_1\frac{e^{-jk[R'_1+r_1]}}{R'_1+r_1}\cos(r_1,n) \tag{6}$$

$$\frac{\partial G}{\partial n}=-jk\frac{e^{-jkR_2}}{R_2}\cos(R_2,n)-jk\ \rho\ \mathrm{Div}_2\frac{e^{-jk[R'_2+r_2]}}{R'_2+r_2}\cos(r_2,n). \tag{7}$$

Substitution of (3), (4), (6), and (7) into (1), yields the sum of four terms, the first one being exactly the same as when the obstacle is a conducting half plane. This term is called knife edge term. It is characterized by the path of radiation $T_1 V\ T_2$.

The other terms which are called halo terms, can be characterized in a similar manner by the paths of radiation which are $T_1 S_1 V\ T_2$, $T_1 V\ S_2 T_2$, $T_1 S_1 V\ S_2 T_2$. It is seen that the treatment of the problem is very similar to what is generally known as four-ray-theory [9] of a knife edge obstacle over plane conducting ground. In that theory the factors ρ have different values for parallel and perpendicular polarization. For a perfectly conducting plane earth,

$$\rho_{\parallel} = -1 \tag{8}$$

$$\rho_{\perp} = +1 \tag{9}$$

Since geometrical optics has been used to calculate the field reflected by the obstacle it would appear that the same values must be used for ρ in connection with the present theory. However, a better approximation can be obtained based on the succeeding arguments.

As mentioned at the beginning of this section, a correct value for E would be obtained from (1) if the correct field values of E' were known in plane Ξ. Instead the values of the incident field are substituted for E'. In the analogous case of diffraction by a circular aperture, Braunbek [10] could improve the results by adding, to the incident field, field values near the rim of the aperture which he derived from Sommerfeld's [11] electromagnetic theory of the diffraction field near the straight edge of an infinite half-plane. The same approach has been used by H. Levine [12] in his treatment of the same problem.

In the present case of scattering by a cylindrical obstacle a similar improvement can be obtained when electromagnetic theory of scattering by a conducting cylinder is combined with the observation that the main contributions to the integrals representing the halo terms are supplied by rays that are almost grazing. [1].

From Fock's [13] investigations it is known that, in the case of perpendicular polarization, the electric field at the grazing point is very nearly 1.4 times the incident field, whereas straight geometrical optics would yield a factor of two in agreement with (9). Hence, it is to be expected that

$$\rho_{\perp} = 0.7 \tag{10}$$

leads to a better agreement with experimental evidence than $\rho_{\perp} = 1.0$.

This reasoning is unsatisfactory only in one respect. It cannot be applied to the case of parallel polarization because the total field at the surface of a perfect conductor is zero whether it is calculated by geometrical optics or by electromagnetic theory. Hence, any finite value could be chosen for $\rho_{\parallel}$. The only justification for setting

$$\rho_{\parallel} = -1.0$$

is that it is the simplest assumption and that it leads to good agreement with experimental results. However, a slightly smaller value than 1.0 might produce an even better agreement.

Strictly speaking ρ is not a constant but depends on the location of the point of the surface where the reflection takes place. Thus, the incident field yielding the knife edge term would also have to be multiplied by a similar factor ρ' since the strength of this field is also reduced very near the top of the obstacle where, for perpendicular polarization, $\rho' = \rho = 0.7$. Since the zone of the plane of integration where $\rho' \neq 1$ is narrow compared with the first Fresnel zone the factor ρ' can be set equal to unity for the calculation of the knife edge term. On the other hand, the first "Fresnel zone" in the calculation of the halo terms is so small that ρ can be set equal to the constant value 0.7. It has been shown [14] that the agreement between theory and experiment can be slightly improved by calculating the halo terms with a varying ρ factor.

3. Detailed Theory

The general theory of the previous section may now be applied to generalize the earlier results [1, 2] in two directions: (a) The mountain may have a top that is more appropriately described by a cone. (b) Electromagnetic radiation is incident under an angle that may be different from 90 degs.

An approximate description of the obstacle would be that of a cone with a fairly small cone angle, with its axis more or less horizontal, and with its circular base approximately vertical. The tip of the cone is, in general, far away from the point where the radiation crosses the obstacle (fig. 2).

The theory will be general enough to cover also another case of great practical interest (fig. 3). The base of the cone is essentially horizontal, its axis approximately vertical, and the radiation is diffracted around the obstacle at two opposite sides. In this case the cone angle is, in general, fairly large.

It may be mentioned that the picture of "creeping waves" is not commensurate with this theory. As is typical for Huygen's Principle, all the rays from the source reaching the plane of integration, either directly or after reflection, generate secondary radiation. The sum of all these secondary wavelets at the receiver is the field E of eq (1). Hence, the question for the path of radiation along the surface of the scatterer is not meaningful in this theory.

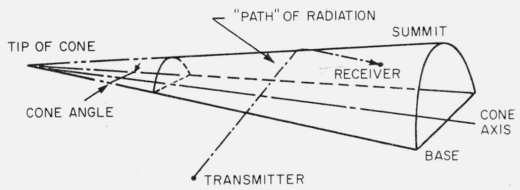

FIGURE 2. *Diffraction by a conical obstacle where radiation travels around one side of the cone.*

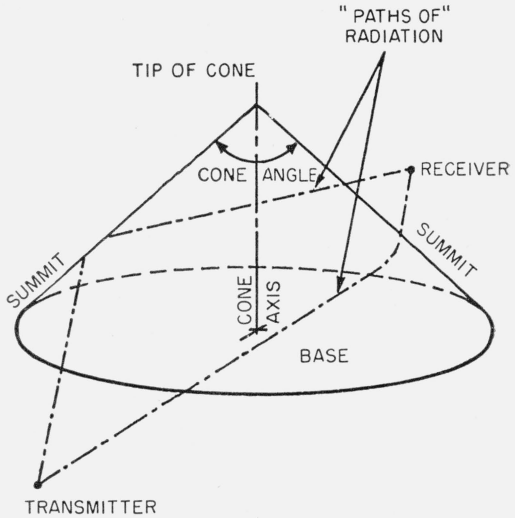

FIGURE 3. *Diffraction by a conical obstacle where radiation can travel around both sides of the cone.*

3.1. Knife Edge Term

The knife edge term corresponds to the "direct" path of radiation ($T_1V\,T_2$) and is obtained by replacing the obstacle by a conducting half-plane. For the situation of figure 2, the resulting obstacle is a simple, rectangular knife edge for which the solution is well known. The knife edge obstacle for the case of figure 3, represents a plane obstacle of triangular shape. The diffraction of electromagnetic waves by such an obstacle will be dealt with in the sequel.

Figure 4 represents a plane conducting obstacle of triangular shape as seen from the transmitter T. The straight line connecting transmitter T and receiver T_2, intersects the obstacle at B. The obstacle is subdivided into five different areas whose effects are calculated separately and by different methods.

Lines b and b' are drawn, through B, parallel to the edges a and a' of the obstacle. They include the angle ϕ. Lines BC and BC' are perpendicular to a and a' respectively. Finally

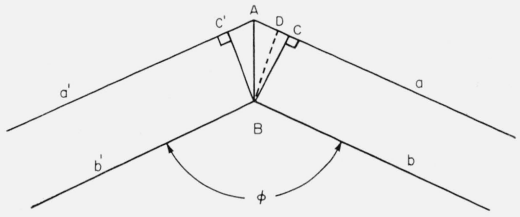

FIGURE 4. *Subdivision of triangular region into five different areas.*

A and B are connected by a straight line. Temporarily it is assumed that TT_2 is perpendicular to the plane of the obstacle. This simplifying assumption will be dropped later.

If there is no obstacle the total unobstructed field radiated from T towards T_2 is well known. The field intercepted by the obstacle can be calculated by means of Kirchhoff's formula and subtracted from the total field (Babinet's Principle). For this purpose the obstacle is subdivided into: (1) The triangular area, of infinite extent, bounded by b and b'; (2) the two rectangular areas bounded by a, b, and BC and by a', b', and BC'; and (3) the two triangles ABC and ABC'.

The contribution of the triangular area bounded by b and b' is $\phi/2\pi$ of the total field. This follows immediately from Kirchhoff's formula. The total field without obstacle is given by

$$E_{\text{total}}=\frac{jk}{4\pi}\int_0^{2\pi}\int_0^{\infty}\frac{e^{-jk(R_1+R_2)}}{R_1R_2}(\cos\theta_1-\cos\theta_2)\,\rho\,d\rho\,d\phi \tag{11}$$

where: the integration is extended over the entire plane, ρ, ϕ are cylindrical coordinates with origin at B. As usual, R_1 and R_2 are the distances from T to the element of integration and from there to T_2. θ_1 and θ_2 are the angles of incidence. When a triangular obstacle bounded by b and b' is present, the upper limit of the first integral of eq (11) is $(2\pi-\phi)$ instead of 2π. Since the integrand is independent of ϕ, eq (12) is obtained.

$$E=E_{\text{total}}-\frac{\phi}{2\pi}E_{\text{total}}. \tag{12}$$

The effect of the rectangular areas can be calculated by exactly the same method used in the well known treatment of Fresnel diffraction by a half plane. For normal incidence it is found that the effect of the rectangular area bounded by the straight lines a, b, and BC, is given by

$$E_{\text{rect.}}=e^{-jkd_m}\cdot\left(\frac{1+j}{4d_m}\right)\left[\left(C\sqrt{\frac{2k}{\pi d_m}}\,c\right)-jS\left(\sqrt{\frac{2k}{\pi d_m}}\,c\right)\right] \tag{13}$$

where C and S are Fresnel's cosine and sine integrals, the meaning of c is explained by figure 5, and that of d_m by eq (18).

To obtain the "knife edge" term of the scattered field it is necessary to subtract, from the right-hand side of eq (12), the expression (13), with a corresponding one for the other rectangular area and expressions for the effect of the two finite triangular areas ABC and ABC'. Triangle ABC may be treated as example. The angles of incidence can be considered constant when the dimensions c and s of the triangle (fig. 5) are small compared to the distance d_1 and d_2 of the stations from point B. For perpendicular incidence, $\theta_1=\theta_2-\pi=0$. The (negative) contribution of the triangle is

$$E_{\Delta}=\frac{jk}{2\pi d_1d_2}\iint e^{-jk(R_1+R_2)}\,d\sigma \tag{14}$$

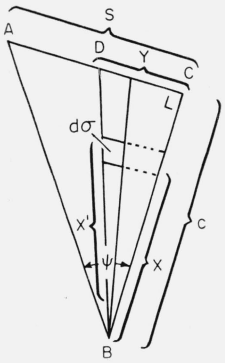

FIGURE 5. *Notation for evaluating contribution of area* A B C.

where,

$$d\sigma=\frac{x}{c}\,dy\,dx. \tag{15}$$

Making the substitution:

$$R_1+R_2=d+\frac{x^2}{d_m}\,(1+y^2/c^2) \tag{16}$$

with

$$d=d_1+d_2; \tag{17}$$

$$2/d_m=1/d_1+1/d_2 \tag{18}$$

and integrating with respect to x, we obtain:

$$E_\Delta=\frac{e^{-jkd}}{2\pi dc}\int_0^s \frac{dy}{1+y^2/c^2}\left[1-e^{-jk\frac{c^2}{d_m}(1+y^2/c^2)}\right]. \tag{19}$$

The integral splits up into the difference of two integrals. The second one is evaluated by the stationary phase method yielding

$$E_\Delta=\frac{e^{-jkd}}{2\pi dc}\left[c\psi-\sqrt{\pi d_m/2k}\;e^{-\left(jk\frac{c^2}{d_m}\right)}\left\{C(\sqrt{2k/\pi d_m}\,s)-jS(\sqrt{2k/\pi d_m}\,s)\right\}\right]. \tag{20}$$

Minor changes take place when the plane of the obstacle is not perpendicular to the straight connection TT_2. For the succeeding derivations it is assumed that the decisive contribution to the integrals in question are made by surface elements $d\sigma$ whose distance ρ from B is small compared to d_1 and d_2 so that the angle of incidence ζ can be considered constant for the integration, ζ being the angle between TT_2 and the perpendicular of the plane of the obstacle. With this assumption, the integrand of eq (11) can be written

$$2\,\frac{e^{-jk(R_1+R_2)}}{R_1R_2}\cos\zeta d\sigma. \tag{21}$$

The product $\cos\zeta\;d\sigma$ can be replaced by $d\sigma'$ where $d\sigma'$ is the surface element obtained by projection of $d\sigma$ onto a plane perpendicular to TT_2.

Figure 6 represents a plane through the stations T, T_2, and through the element of integration $d\sigma$. The distance of $d\sigma$ from B is ρ. Depending on the location of $d\sigma$ in the plane of the obstacle, angle Ω assumes a value between $\pi/2-\zeta$ and $\pi/2+\zeta$. An elementary calculation yields

$$R_1+R_2=d_1+d_2+(\rho^2/d_m)\sin^2\Omega.$$

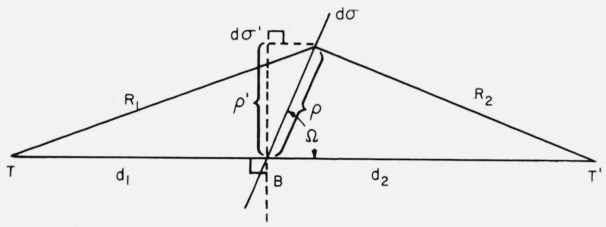

FIGURE 6. *Plane through station* TT′ *for calculation of effect of oblique incidence on triangular obstacle.*

Denoting the distance of $d\sigma'$ from B by $\rho'=\rho \sin \Omega$ we can replace (21) by

$$2 \frac{e^{-jkd}}{d_1 d_2} e^{-jk\rho'^2/d_m} d\sigma'. \tag{22}$$

This expression establishes the rule that a plane oblique obstacle must be projected onto a perpendicular plane and that the diffraction field must be calculated as if the projection were the obstacle.

3.2. Halo Terms

The halo terms represent the additional radiation due to the smooth surface of the obstacles rather than the sharp edges of their plane substitutes. The following derivations will be based more on the situation of figure 2, rather than figure 3, although the theory applies to both cases.

If a_c is the radius of curvature, it will be assumed that $ka_c >> 1$. This would exclude the area near the tip of the cone which may be important in the case of figure 3. The halo terms obtained for the cylindrical mountain in the earlier publications [1, 2]tend towards zero with vanishing a_c in agreement with experiment. Since this theory will lead to a similar result we feel certain that it can be applied to any part of the cone, be it near its tip or far away from it, although $ka_c >> 1$ is a basis of its derivation.

Experimental evidence does not indicate the existence of a special contribution of the tip of the cone of any appreciable amount. This is in agreement with the general experience that a point singularity does not contribute appreciably to the far field.

It is understandable that the mathematical expression will be more involved for oblique incidence on a conical mountain than for normal incidence on a cylindrical mountain, the latter being a special case of the former. The more important difference, however, is that the integral over the mathematical plane which is typical of Huygen's principle, reduces immediately to a simple integral in the cylindrical case whereas the double integral must be treated much more carefully in the conical case.

The reason is that the situation of the point of stationary phase for the integration parallel to the cylinder axis is self evident. For the conical obstacle and oblique incidence, the point of stationary phase must be determined by a rather laborious calculation. This will be described in several steps.

a. Geometrical Preliminaries

Following notations will be used: Point 0 is the tip of the cone; cone angle is 2τ; and transmitter and receiver are located at points T_1 and T_2, respectively.

Two tangential planes, one through T_1 and another one through T_2, touch the cone in the generatrices OU_1 and OU_2 where the exact location of points U_1 and U_2 along the generatrices will be determined later. The two tangential planes T_1OU_1 and T_2OU_2 intersect in a straight line ON. The plane through the cone axis and through ON will be used as plane Ξ of integration in the sense of Huygen's principle. A third tangential plane is perpendicular to Ξ and is used as base plane.

Figure 7 shows a ground plan of stations and conical obstacle. This figure is obtained by projection onto the base plane. The projections of points onto the base plane are marked by brackets added to the notation of the corresponding points. The straight connection of points (T_1) and (T_2) intersects the plane of integration in A so that OA is the generatrix that lies in the base plane. The acute angle between $(T_1)A$ and the perpendicular to OA is called "angle of incidence ζ." The lengths of $\overline{T_1(T_1)}$ and $\overline{T_2(T_2)}$ are denoted h_1 and h_2 (fig. 8). They are taken positive for points under the base plane.

A plane through A and perpendicular to the cone axis intersects the cone in a circle whose center is M and whose radius is a. Points U_1, U_2, and N are located in this plane.

It is assumed that the distance $d_1=\overline{(T_1)A}$ and $d_2=\overline{(T_2)A}$ are large compared to a,

$$d_1>>a; \qquad d_2>>a. \tag{23}$$

A right-handed rectangular coordinate system with origin in 0 is used. The positive z-axis is OA, the x-axis lies in the base plane, the y-axis in the plane of integration, $OMAN$.

Figure 8 shows an intersection with the plane MU_1AU_2 which is perpendicular to the cone axis. We set

$$\angle AMU_1=\angle AMU_2=\psi_0 \tag{24}$$

Another point on the circumference of the circle is denoted S_1 and,

$$\angle U_1MS_1=\psi. \tag{25}$$

A ray transmitted from T_1 and incident at S_1 is reflected by the cone so that it intersects the plane of integration, $x=0$, in V. Ray S_1V seems to come from the image T_1' of point T_1. Points T_1 and T_1' are symmetrical to the tangential plane through generatrix OS_1. (In general, none of the points T_1, T_1', V lies in the plane of fig. 8.)

Any other ray transmitted from T_1 and incident at one of the points of generatrix OS_1, is reflected as if it comes from T_1' and intersects the plane of integration in a point of the straight line OV.

Generatrix OA will be called summit of the mountain. The radius of curvature of the mountain at point A is obtained by putting a plane perpendicular to the summit through A, which intersects the cone axis in the center of the osculating circle M'. Hence, the radius of curvature in this cross section is $z_0 \tan \tau=a/\cos \tau$. The radius of curvature in the cross section of a plane through T_1AT_2 (which contains also M') is

$$a_c=a/(\cos \tau \cos \zeta). \tag{26}$$

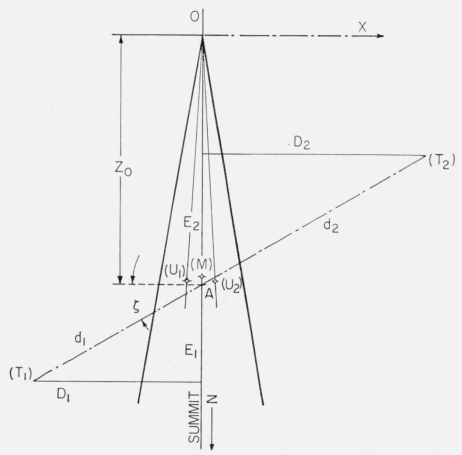

FIGURE 7. *Plan view of stations and conical obstacle.*

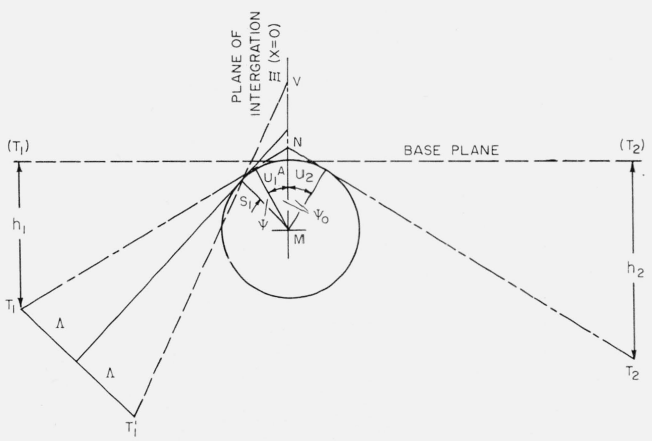

FIGURE 8. *View in plane perpendicular to cone axis.*

The angles of incidence occurring in eqs (6) and (7) can be approximated by ζ or $\pi+\zeta$, respectively. Substituting (3), (4), (6), and (7) into (1), we obtain

$$E=\frac{jk}{4\pi}\{e_0+\rho e_1+\rho e_2+\rho^2 e_{12}\} \tag{27}$$

where e_0, e_1, e_2, e_{12} are integrals characterized by the paths of radiation T_1VT_2, $T_1S_1VT_2$, $T_1VS_2T_2$, $T_1S_1VS_2T_2$. Being slowly varying functions the distances R_1, $R_1'+r_1$, R_2, $R_2'+r_2$ in the denominators of (3), (4), (6), and (7) can be approximated by d_1 and d_2, respectively.
Hence,

$$e_0=\frac{2\cos\zeta}{d_1d_2}\iint e^{-jk[R_1+R_2]}\,dS \tag{28}$$

$$e_1=\frac{2\cos\zeta}{d_1d_2}\iint e^{-jk[R_1'+r_1+R_2]}\,dS \tag{28'}$$

$$e_{12}=\frac{2\cos\zeta}{d_1d_2}\iint e^{-jk[R_1'+r_1+R_2'+r_2]}\,dS. \tag{28''}$$

The expression for e_2 is obtained from (28') by an exchange of subscripts "1" and "2".

b. Determination of the point of stationary phase

In this subsection a series of calculations will be briefly described which are required for the evaluation of the integrals (28') and (28''). The integral for e_1 will be considered in particular.

Point V has been obtained by reflection of radiation at point S_1, another point V' is obtained by reflection at a slightly different point whose corresponding angle is $\psi+d\psi$ instead of ψ.

The double integral for the summation of the contribution of all the wavelets is carried out in two steps, first a simple integral over a narrow triangular strip VOV' which extends to infinity beyond V and V', followed by another simple integral over the different strips from $\psi=0$ up.

The integration over one strip is done by the stationary phase method. The point of stationary phase is obtained by putting a plane through OV and T_2 and folding it up by tilting it about OV until it coincides with plane OVT_1'. By this operation point T_2 is brought to T_2^*. The straight line $T_1'\,T_2^*$ intersects OV at the point of stationary phase and the length of $\overline{T_1'\,T_2^*}$ determines the phase of the radiation arriving from T_1 at T_2 after reflection from the cone and reradiation.

The details of the calculations shall not given here.[4] They are simplified by the assumption of small scattering angles so that powers of higher than first order in ψ_0 are neglected. From the corresponding calculations [1] for normal incidence on cylindrical mountains it is concluded that powers up to the third in ψ must be carried. Mixed terms in $\psi_0\,\psi^3$ have been disregarded as the numerical calculations for the cylinder [1] have shown that their effect on the result is negligible.

c. Evaluation of the Integrals

The substitution (29) can be made in the exponent of eq (28'),

$$R_1'+r_1+R_2=\text{Dist}\ (T_1'T_2^*)+\delta\ \text{Dist}\ (T_1'T_2^*). \tag{29}$$

It can be shown that [4]

$$R_1'+r_1+R_2=\text{Dist}\ (T_1'T_2^*)+\frac{\cos^2\zeta}{d_m}\,\delta\xi^2. \tag{30}$$

[4] For details, see: RCA Victor Research Rept. No. 7-100, 4.

When corresponding substitutions are made in (28) and (28'') the eqs (31), (32), and (33) are obtained.

$$e_0=2\frac{\cos\zeta}{d_1d_2}\iint\exp\left[-jk\left\{\text{Dist }(T_1VT_2)+\frac{\cos^2\zeta}{d_m}\delta\xi^2\right\}\right]dS \tag{31}$$

$$e_1=2\frac{\cos\zeta}{d_1d_2}\iint\text{Div }(S_1)\exp\left[-jk\left\{\text{Dist }(T_1'T_2^*)+\frac{\cos^2\zeta}{d_m}\delta\xi^2\right\}\right]dS \tag{32}$$

$$e_{12}=2\frac{\cos\zeta}{d_1d_2}\iint\text{Div }(S_1)\,\text{Div }(S_2)\exp\left[-jk\left\{\text{Dist }(T_1'T_2'^*)+\frac{\cos^2\zeta}{d_m}\delta\xi^2\right\}\right]dS. \tag{33}$$

The integration of the factor of (32) that depends on ξ' where:

$$\xi'=\sqrt{\frac{2k}{\pi d_m}}\cos\zeta\,d\xi$$

is achieved by the stationary phase method.

$$\int_{-\infty}^{\infty}\sqrt{\frac{\pi d_m}{2k}}\frac{1}{\cos^2\zeta}\exp\left(-\frac{jk}{d_m}\cos^2\zeta\,\delta\xi^2\right)d\xi'=\sqrt{\frac{\pi d_m}{k}}\frac{\exp(-j\pi/4)}{\cos^2\zeta}.$$

Substituting this expression into (32) together with some added manipulations,

$$\frac{jk}{4\pi}e_1=\sqrt{\frac{kd_m}{\pi}}\frac{a_e\exp(j\pi/4)}{2d_1d_2\cos\zeta}\int\sqrt{\chi(3\chi+2\psi_{sc})}\exp[-jk\text{ Dist }(T_1'T_2^*)]d\chi \tag{34}$$

where:

$$\text{Dist }(T_1'T_2^*)=d+2(a_c/\cos\zeta)\chi^3+5(a_c/\cos\zeta)\psi_{sc}\chi^2, \tag{35}$$

and

$$\chi=(\cos\zeta\cos\tau)\psi.$$

Comparison of (34) and (35) with eqs (13b) and (14) through (17) of [1] yields immediately the result that the first halo term is exactly the same in both cases if a is replaced by $a_c/\cos\zeta$ and ψ_0 by ψ_{sc}

The third halo term represented by e_{12} is calculated in a corresponding manner. As has been pointed out [1] the angles ψ on the two sides of the plane of integration are not, in general, equal in magnitude. However, a mean value for ψ is assumed to be sufficiently accurate.

It can be found that

$$\text{Dist }(T_1'T_2'^*)=d+4(a_c/\cos\zeta)\chi^3+7(a_c/\cos\zeta)\psi_{sc}\chi^2. \tag{36}$$

Again a comparison with eqs (21) and (22) of [1] shows that the third halo term is the same if a is replaced by $a_c/\cos\zeta$ and ψ_0 by ψ_{sc}.

A more accurate calculation yields an additional term to the expression (36) for Dist $(T_1'T_2'^*)$,

$$[3\,a_c^2/(d_m\cos^2\zeta)]\,\psi_{sc}\chi^3.$$

d. Correction Factors

A last remark shall be made with respect to the correction factors $\rho_\parallel$ and $\rho_\perp$ which were discussed at the end of section 2. It has still to be shown that $\rho_\perp=+0.7$ also for oblique incidence.

A convenient way makes use of formulas published by J. R. Wait [15, 16]. Wait studies oblique incidence of a plane wave on a cylinder by means of a series expansion. Since he considers the case of parallel polarization, the easiest way of using his equations is to consider the perpendicular component of the magnetic vector H_ρ^s for a cylinder of infinite permeability which behaves like the electric vector for infinite conductivity. With Wait's notations, from Maxwell's equations,

$$-kj\,\eta\,H_\rho^s=\partial E_z^s/\partial(\rho\phi)-\partial E_\phi^s/\partial Z.$$

Substituting from his eqs (3) and (6) for E_z^s and E_ϕ^s and setting $\phi=\pi/2$, $\rho=a$,

$$H_\rho^s=-\frac{E_0}{\eta v}\sum\frac{J_n'(v)}{H_n^{(2)\prime}(v)}H_n^{(2)}(v)\exp\left(-jkz\cos\theta+j\phi t\right)$$

where J_n and $H_n^{(2)}$ are the Bessel and Hankel functions in the usual notations, and his v is, with our notations,

$$v=ka\sin\zeta$$

It follows that,

$$|H_\rho^s|=-\frac{E_0}{\eta v}\left|\sum\frac{J_n'(v)}{H_n^{(2)\prime}(v)}H_n^{(2)}(v)\right|.$$

Fock [13] has investigated the case $\zeta=\pi/2$ and $ka>>1$. He found a numerical value for $|H_\rho^s|/E_0$ which is independent of a. Hence, $|H_\rho^s|/E_0$ is independent of v and, consequently, it is also independent of ζ when $\zeta\neq\pi/2$.

4. Experiment

4.1. Apparatus and Technique

Experimental measurements of power diffracted by smooth half-conical mountains have been performed in the K-band frequency range using model techniques. The details of the experimental arrangement have been discussed previously [1].

Two overlapping, perfectly conducting, conical mountains of 15° half-angle were used in the investigations. The first was connected to a knife edge obstruction with a transition into a 15° cone which extended to a ka of about 200. The second was a complete half-cone and covered the range of $ka=0$ to 400. The knife edge cone transition was used in order to provide an automatic normalization of the received power as a function of effective radius of the cone to the power diffracted by a knife-edge ($ka=0$) obstacle. Thus a continuous plot of diffracted power for different ka values ranging from 0 to 330 was possible by moving the cones perpendicular to the plane joining a fixed transmitter-receiver location before end effects became of consequence. In all measurements the surface of the cone (and the knife edge) was either parallel or perpendicular to the incident electric vector so that cross-polarization effects would not be present.

4.2. Diffraction by Conical Mountains

The power behind a conducting conical mountain as function of ka_c($k=2\pi/\lambda$, $a_c=$ effective radius of the cone in the vertical plane containing both transmitter and receiver) for normally incident ($\zeta=0$) electromagnetic waves at the grazing angle is shown in figure 9. A large difference between the two polarizations exists with the vertically polarized field which increases with radius of curvature being much stronger than the horizontally polarized field which decreases with radius of curvature (ka_c). The measurements agree well with the expression for power at grazing incidence derived earlier.

A complete family of measurements of power variation with ka_c when the electromagnetic energy is normally incident on a conical mountain for different receiver positions (i.e., different scattering angles) is shown in figure 10a, for vertical polarization, and in figure 10b for horizontal polarization.

The variation of power diffracted by a conical obstacle with scattering angle is shown in figure 11. As for a cylindrical mountain, the received power for vertical polarization increases

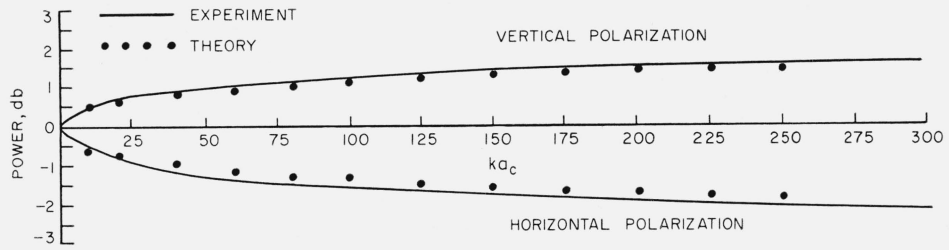

FIGURE 9. *Variation of power behind a conical mountain at grazing incidence with radius of curvature of the obstacle in the vertical plane containing the transmitting and receiving terminals.* (d_1=150λ, d_2=113λ, ψ_0=0°, λ=1.252 cm.)

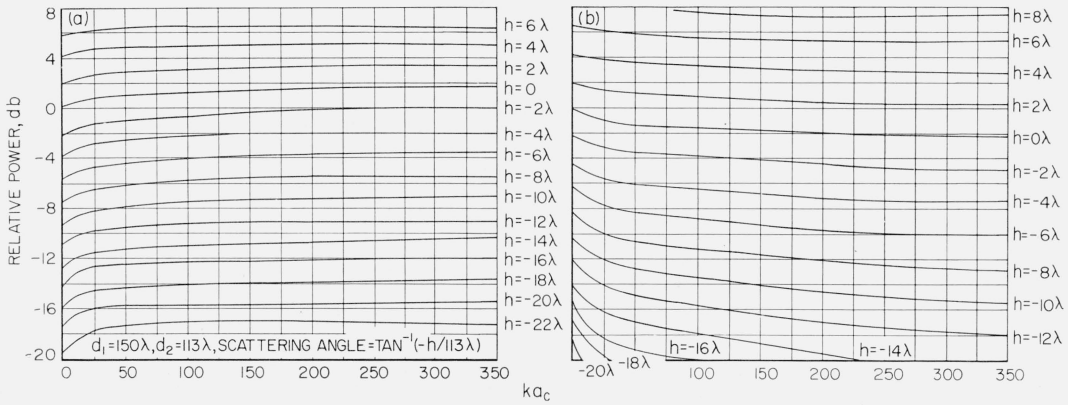

FIGURE 10. *Measured variation of power behind a conical mountain with radius of curvature of the obstacle in the vertical plane containing the transmitting and receiving terminals.*

a, vertical polarization and b, horizontal polarization.

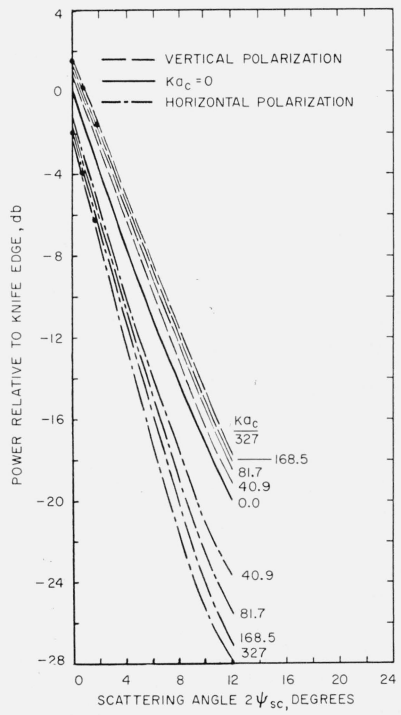

FIGURE 11. *Variation of power behind a conical mountain with scattering angle as a function of radius of curvature.* (d_1=150λ, d_2=113λ, $\psi_{sc}=\psi_0 \cos\tau \cos\zeta$; $a_c=a/\cos\tau\cos\zeta$; τ=15°, ζ=0°.)

Theoretical points are for ka_c=239.

with ka_e, while the reverse is true for horizontal polarization. In addition, the slope of the power variation with scattering (diffraction) angle becomes steeper with increasing curvature for horizontal polarization and remains essentially the same as for a knife edge in the case of vertical polarization. The agreement with theory appears satisfactory.

The power distribution behind a conical mountain for $ka_e=327$ is shown in figure 12. These should be compared to the power variation behind a knife edge obstacle [1]. Calculations of the power for grazing incidence are shown and agree well with the measurements.

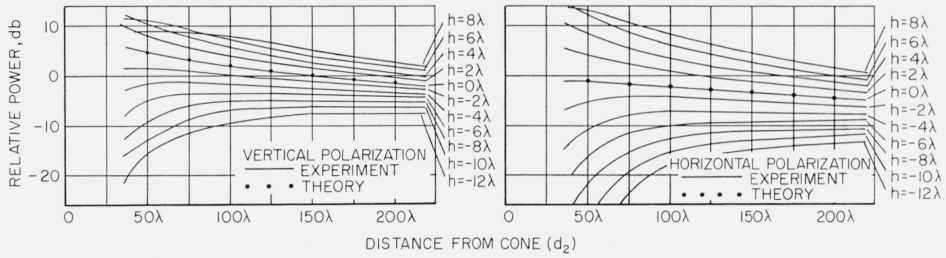

FIGURE 12. *Power distribution behind a conical mountain.*
(k a_e=327, d_1=150λ, λ=1.252 cm.)

The authors thank the Air Force Cambridge Research Center for supporting this work under Contract AF19(604)3049, and M. G. Kingsmill, for performing the experimental measurements.

5. References

[1] H. E. J. Neugebauer and M. P. Bachynski, Diffraction by smooth cylindrical mountains, Proc. IRE **46,** 1619 (1958).

[2] I. P. Shkarofsky, H. E. J. Neugebauer, and M. P. Bachynski, Effect of mountains with smooth crests on wave propagation, IRE Trans., PGAP **AP–6,** 341 (1958).

[3] J. R. Wait and A. M. Conda, Diffraction of electromagnetic waves by smooth obstacles for grazing angles, J. Research NBS **63D**, 181 (1959).

[4] A. Sommerfeld, in Frank-Mises, Die Differential—und Integralgleichungen der Mechanik und Physik, 2d ed. **II,** p. 853 (Braunschweig, 1935).

[5] P. M. Morse and H. Feshbach, Methods of theoretical physics, **I,** p. 812 (McGraw-Hill Book Co., New York, N.Y., 1953).

[6] H. Severin, Zur Theorie der Beugung elektromagnetischer Wellen, Z. Phys. **129,** 426 (1951).

[7] W. Franz, Ueber die Greenschen Funktionen des Zylinders und der Kugel, Z. Naturforsch. **9a,** 705 (1954).

[8] H. J. Riblet and C. B. Baker, A general divergence formula, J. Appl. Phys. **19,** 63 (1948).

[9] J. C. Schelling, C. R. Burrows, and E. B. Ferrell, Ultra-short wave propagation, Proc. IRE **21,** 427 (1933).

[10] W. Braunbek, Neue Näherungs Methode für die Beugung am ebenen Schirm; Zur Beugung an der Kreisscheibe; Z. Physik **127,** 381–390 and 405–415 (1950).

[11] M. Born, Optik, pp. 209–218 (J. Springer, Berlin, 1933).

[12] H. Levine, Aperture diffraction near the geometrical optics limit, McGill Symp. Microw. Optics, pt. II, p. 211 (McGill Univ., Montreal, Canada, June 22 to 25, 1953).

[13] V. Fock, The distribution of currents induced by a plane wave on the surface of a conductor, J. Phys. (USSR) **10,** 130 (1946).

[14] I. P. Shkarofsky, M. P. Bachynski, and H. E. J. Neugebauer, Electromagnetic propagation over mountains, Can. IRE Conv. Record (Oct. 1958).

[15] J. R. Wait, Scattering of a plane wave from a circular dielectric cylinder at oblique incidence, Can. J. Phys. **33,** 189 (1955).

[16] J. R. Wait, Electromagnetic radiation from cylindrical structures (Pergamon Press, New York, N.Y., 1959).

(Paper 64D–64)